Published online 25 May 2007

Nucleic Acids Research, 2007, Vol. 35, No. 11 ***3859–3867***
doi:10.1093/nar/gkm337

Cell cycle regulation as a mechanism for functional separation of the apparently redundant uracil DNA glycosylases TDG and UNG2

Ulrike Hardeland[2,†], Christophe Kunz[1,†], Frauke Focke[1], Marta Szadkowski[3] and Primo Schär[1,*]

[1]Centre for Biomedicine, DKBW, University of Basel, Mattenstrasse 28, CH-4058 Basel, Switzerland, [2]Molecular Metabolic Control, DKFZ, Im Neuenheimer Feld 280, D-69120 Heidelberg, Germany and [3]KuDOS Pharmaceuticals Ltd., 327 Cambridge Science Park, Milton Road, Cambridge, CB4 0WG, UK

Received March 5, 2007; Revised April 18, 2007; Accepted April 19, 2007

ABSTRACT

Human Thymine-DNA Glycosylase (TDG) is a member of the uracil DNA glycosylase (UDG) superfamily. It excises uracil, thymine and a number of chemical base lesions when mispaired with guanine in double-stranded DNA. These activities are not unique to TDG; at least three additional proteins with similar enzymatic properties are present in mammalian cells. The successful co-evolution of these enzymes implies the existence of non-redundant biological functions that must be coordinated. Here, we report cell cycle regulation as a mechanism for the functional separation of apparently redundant DNA glycosylases. We show that cells entering S-phase eliminate TDG through the ubiquitin–proteasome system and then maintain a TDG-free condition until G2. Incomplete degradation of ectopically expressed TDG impedes S-phase progression and cell proliferation. The mode of cell cycle regulation of TDG is strictly inverse to that of UNG2, which peaks in and throughout S-phase and then declines to undetectable levels until it appears again just before the next S-phase. Thus, TDG- and UNG2-dependent base excision repair alternates throughout the cell cycle, and the ubiquitin–proteasome pathway constitutes the underlying regulatory system.

INTRODUCTION

Uracil (U) arises in DNA either by erroneous incorporation of dUMP opposite adenine (A) during DNA synthesis or by deamination of cytosine (C), which generates a U mispaired with guanine (G). To what extent A•U base pairs affect the function of DNA is unclear; G•U mispairs, however, give rise to C → T mutations if a DNA polymerase replicates across. Uracil DNA glycosylases (UDGs) (1) have evolved to eliminate this irregular base from the DNA. They hydrolyze the *N*-glycosidic bond linking the U to the sugar moiety of the nucleotide, thereby initiating a base excision repair (BER) process (2) that restores the canonical Watson–Crick base pair. Mammalian cells posses at least four enzymes with UDG activity, namely UNG, TDG, SMUG1 and MBD4 (3–6), and the successful co-evolution of these enzymes implies that each of them fulfils specific non-redundant biological functions. The question then is how cells achieve the functional separation of these enzymatically redundant activities. One way would be to control their spatial and temporal distribution as exemplified by the UNG proteins. Differential expression of the human *UNG* gene from two alternative promoters generates two isoforms, UNG1 and UNG2, that localize to mitochondria and to nuclei, respectively (7). Moreover, *UNG2* expression is up-regulated during S-phase of the cell cycle where the protein associates with PCNA and RPA at replication foci, implicating a role for this UDG in the removal of misincorporated U during DNA replication (8,9). Whether similar forms of regulation apply to other UDGs and, thus, could provide a cellular mechanism for functional coordination of uracil repair is not known. Here, we report that Thymine-DNA Glycosylase (TDG), a mismatch-specific UDG, underlies strict cell cycle regulation. TDG has a comparably broad substrate spectrum including the deamination product of 5-methylcytosine, i.e. a T mispaired with a G, but its most efficiently processed physiological substrate is a G•U mispair (6). Cells entering S-phase eliminate this glycosylase through the ubiquitin–proteasome pathway and

*To whom correspondence should be addressed. Tel: +41 0 61 267 0767; Fax: +41 0 61 267 3566; Email: primo.schaer@unibas.ch

†The authors wish it to be known that, in their opinion, the first two authors should be regarded as joint First Authors.

maintain a TDG free state until DNA replication is completed. Degradation of TDG is critical for S-phase progression and cell proliferation, implicating that this UDG interferes negatively with vital processes of DNA replication. Strikingly, TDG levels decline just when UNG2 expression comes up and *vice versa*, suggesting that uracil repair is handled by distinct pathways throughout the cell cycle that are coordinated by the ubiquitin–proteasome system.

MATERIAL AND METHODS

Reagents and antibodies and expression constructs

The complete^{TM} protease inhibitor tablets were purchased from Roche (Switzerland). All other chemicals and reagents were from Sigma (Germany). All media and supplements used for cell culture were purchased from Gibco BRL (Invitrogen, UK). The polyclonal and monoclonal (99) anti-TDG antibodies were described earlier (Hardeland *et al*., 2002), anti-ubiquitin (P4D1) and anti-cyclin B1 (GNS 1) antibodies were from Santa Cruz Biotechnology, Inc. (CA, USA), anti-HA (3F10) antibody from Roche (Switzerland), anti cyclin A (BF 683) from Milliporee (MA, USA) and anti-cyclin E (Ab-1, Ab-2) antibodies from Labvision (CA, USA), and anti-UNG (ab23926) and anti MBD4 (ab12187) antibodies from Abcam (UK). The anti-β-tubulin antibody (N37) and the secondary horse-radish-peroxidase conjugated antibodies were purchased from GE Healthcare Life Sciences (Germany). The plasmid constructs expressing HA-TDG or HA-TDG^{N140A} have been previously described (10).

Cell culturing, cell cycle synchronizations, protein extractions

MRC5 cells were cultured in Nutrition Mix Ham's F-10 medium with Glutamax I, HeLa, HeLa S3 and 293T cells were grown in Dulbecco's modified Eagle's (DMEM) medium containing 2 mM L-glutamine, both supplemented with 10% fetal calf serum and antibiotics (penicillin/streptomycin). For HeLa cells stably or transiently transfected with TDG expression constructs, the medium was supplemented with 0.8 or 0.2 μg/ml puromycin, respectively. Stably transfected 293T cells were grown in the presence of 1.5 μg/ml puromycin. All cultures were incubated at 37°C in a humidified atmosphere containing 5% CO_2. All transfections were done at 30% confluency with 1 μg (HeLa cells) or 8 μg (293T cells) of vector DNA using the Fugene reagent (Roche, Switzerland). The efficiency of plasmid delivery was estimated by transfection of pEGFP-N1 (Clontech, USA) under identical conditions and quantitation of EGFP positive cells by fluorescence microscopy. Transiently transfected cells were cultured for 48 h unless stated otherwise.

For cell cycle analysis, 293T cells were seeded onto microscope slides at a confluency of 50% and allowed to attach for 7 h in medium at 37°C. The slides were then washed three times in PBS and cells fixed in acetone for 2 min at −20°C. After short rehydration with PBS, the slides were covered with staining solution (50 μg/ml propidium iodide, 200 μg/ml RNaseA) and incubated for 30 min at 37°C in a humidified chamber. After quick rinsing in PBS, the slides were covered with 50% glycerol in PBS and a coverslip and their DNA content analysed on a laser scanning cytometer, LSC-1 (LSC® CompuCyte, USA). In parallel, cell cycle analyses were done by standard flow cytometry.

Cell cycle arrest experiments were performed by treatment of 5×10^6 HeLa cells at 50% confluency with either 2.5 mM hydroxyurea (HU, 2 M stock in H_2O), 0.8 μg/ml nocodazole (NO, 1 mg/ml stock in DMSO) or respective amounts of DMSO only. After 16 h, denaturing extracts were prepared by scraping cells from the culture plates in 400 μl of lysis buffer I (8 M urea, 200 mM DTT, 120 mM Tris/HCl pH 6.8, 4% SDS, 20% glycerol, 0.01% bromphenolblue) and heating for 10 min at 95°C. Equal sample volumes were then analysed by 10% SDS–polyacrylamide-gel-electrophoresis (SDS-PAGE) and western blotting. HeLa S3 cells were synchronized by harvesting and reseeding detached mitotic cells as follows. Cells were first cultured to 70% confluency in 8 flasks of 175 cm^2 size. To remove all loosely attaching cells, the cultures were extensively washed with pre-warmed medium. The washing procedure was repeated after another 2 h of incubation. After further 2 h, the medium containing detached mitotic cells was removed and cells collected by centrifugation. 1.3×10^6 cells per time point were replated and grown for the times indicated. At each time point, cells were washed with 1× PBS pH 7.4 on the plate and the proteins extracted by direct lysis in 200 μl lysis buffer I. Equal amounts of extract were then analysed by SDS-PAGE and western blotting. MRC5 cells were synchronized by serum starvation followed by mimosine treatment as described in (11). After release, samples were taken at different time points and cell extracts prepared for western blotting (11).

For proteasome inhibition 5×10^6 HeLa cells at 50% confluency were treated for 12 h with 20 μM MG132 (20 mM stock in DMSO) or an equivalent of DMSO only. The cells were then washed with PBS and directly lysed by addition of 400 μl lysis buffer I. For the preparation of soluble and insoluble protein fractions 2.5×10^7 MG132 treated cells were lysed with 2 ml of lysis buffer II (50 mM Na-phosphate pH 8.0, 125 mM NaCl, 1% NP-40, 0.5 mM EDTA, 1 mM PMSF, 1× complete^{TM} protease inhibitors). Soluble and insoluble proteins were then separated by centrifugation for 15 min at 14 000 r.p.m., 4°C. After removal of the supernatant (soluble proteins) the pellet (insoluble proteins) was resuspended in the same volume. Equal amounts of both fractions were separated by SDS-PAGE and analysed by western blotting. Denaturing extracts of MG132 treated cells were obtained by scraping cells from culture dishes in lysis buffer III (50 mM Tris/HCl pH 7.5, 1% SDS, 5 mM DTT) and heating the suspensions for 10 min at 95°C.

Immunoprecipitation and western blotting

M-280 tosylactivated Dynabeads (Invitrogen, UK) were coated with affinity purified rabbit polyclonal anti-TDG antibody or BSA according to the manufacturer's protocol. An aliquot of 400 μl of the denaturing extracts of MG132 treated HeLa cells was diluted 1:10 in dilution

buffer (50 mM Tris/HCl pH 7.5, 120 mM NaCl, 5% glycerol, 1% NP-40, 1 mM EDTA, 1 mM PMSF and 1× complete™ protease inhibitors) before the addition of equilibrated Dynabeads (~2.4×10^7 beads/assay). After incubation for 4 h at 4°C under rotation, unbound proteins were removed and the beads washed three times with dilution buffer at 4°C. Bound proteins were then eluted in 40 µl of 2× SDS-sample-buffer (200 mM DTT, 120 mM Tris/HCl pH 6.8, 4% SDS, 20% glycerol, 0.01% bromphenolblue) and incubation at 95°C for 5 min. Following protein separation by 8 or 10% SDS-PAGE, western blotting was done with antibodies against TDG and ubiquitin following standard procedures. All antibodies were diluted in TBS-T (100 mM Tris/HCl pH 8.0, 150 mM NaCl, 0.1% Tween20) containing 5% dry milk as blocking reagent; the polyclonal anti-TDG antiserum was diluted 1:10 000, the monoclonal anti-TDG and anti-ubiquitin antibodies 1:1000. Detection of the signals was carried out using the enhanced chemiluminescent (ECL™) substrate system (GE Healthcare Life Sciences, Germany).

Immunofluorescence

HeLa cells were grown on coverslips to a confluency of 30%. After washing extensively in PBS, the cells were fixed for 5 min in pre-chilled methanol (−20°C), re-hydrated for 4 times 10 min at room temperature (rT) in PBS, and permeabilized for 5 min in ice-cold P-buffer (PBS, 0.2% TritonX100). To reduce autofluorescence, the coverslips were incubated for another 5 min in ice-cold P-buffer containing 0.2% $NaBH_4$. Soluble protein was then washed out by gently shaking the coverslips in PBS for 10 min at rT. After blocking for 10 min at rT in hybridization buffer (PBS, 1% BSA), samples were hybridized with affinity-purified polyclonal rabbit anti-TDG- (1:100 dilution) and a FITC coupled anti-PCNA (1:500, Leinco Technologies, MO, USA) antibodies at 4°C overnight. After four washing steps of 10 min in hybridization buffer at rT, samples were hybridized with an anti-rabbit IgG Alexa-546 conjugated secondary antibody (1:200, Invitrogen, UK) at rT for 1 h. After four washing steps of 10 min in PBS, the coverslips were dried and embedded in Mowiol containing 1 µg/ml DAPI. TDG and PCNA signals were visualized on a Axiovert 200M microscope (Zeiss, Germany) using TRITC (exitation 560 nm, emission 580 nm) and FITC (exitation 490, emission 520 nm) filters, respectively.

Northern blot analyses

Total RNA was isolated from MRC5 cells using the TRIzol reagent. RNA concentrations were determined by A_{260} measurement and the quality was checked by electrophoresis on 1% formaldehyde agarose gels. Twenty microgram of total RNA in formamide loading buffer were separated in a 1% agarosegel containing formaldehyde. After washing the gel twice for 10 min in 8 mM NaOH, the RNA was transferred to a Zeta Probe membrane (BioRad, CA, USA) overnight in 8 mM NaOH. After a brief washing step with 2× SSC the transferred RNA was fixed by baking at 80°C. Following pre-hybridization of the membrane at 65°C in hybridization buffer (0.5 M Na_2PO_4 pH 7.2, 7% SDS) for 5 min, hybridization with probe was done for 20 h at 65°C. A ^{32}P-labeled PCR fragment (Megaprime Kit, GE Healthcare Life Sciences, Germany), representing the 5′ part of the TDG cDNA served as specific probe. After hybridization the membrane was washed twice with wash buffer I (40 mM Na_2PO_4 pH 7.2, 5% SDS) for 20 min at 65°C, followed by one washing steps with wash buffer II (40 mM Na_2PO_4 pH 7.2, 1% SDS) at 65°C for 10 min. After exposition of the membrane to a phosphoimager screen, signals were visualized on a Storm phosphoimager (GE Healthcare Life Sciences, Germany).

Ubiquitylation *in vitro*

In vitro ubiquitylation reactions were performed with the ubiquitin conjugation Enzyme Kit (Biotrend, Germany) according to the manufacturer's instructions. An aliquot of 20 µl reactions contained 1× MgATP, 5 µg conjugating fraction I, 5 µg conjugation fraction II, 26 µg ubiquitin (Biotrend), 200 ng ubiquitin-aldehyde and 10 ng of recombinant TDG protein. The reactions were incubated at 37°C for 0 and 2 h and stopped by the addition of 4 µl 6× SDS-sample buffer (600 mM DTT, 360 mM Tris/HCl pH 6.8, 12% SDS, 60% glycerol, 0.03% bromphenolblue). After heating at 95°C for 5 min the reaction products were analysed by 7.5% SDS-PAGE and western blotting with the polyclonal anti-TDG antibody.

Base release assays

Nuclear extracts were prepared from 10^8 HeLa cells harvested after HU (or mock) treatment. Cells were resuspended in ice-cold hypotonic buffer (20 mM HEPES pH 8.0, 5 mM KCl, 1.5 mM $MgCl_2$, 0.5 mM PMSF, 1 mM DTT, 1× complete™ protease inhibitors) at a cell density of 1×10^8 cells/ml and allowed to swell for 20 min on ice. Cells were broken up in a Dounce homogenizer on ice to achieve >80% lysis and the liberated nuclei were harvested by centrifugation at 3000*g* and 4°C. After estimation of the packed nuclear volume (pnv) the pellet was resuspended in 1/2 pnv low salt buffer (20 mM HEPES pH 8.0, 25% glycerol, 1.5 mM $MgCl_2$, 20 mM KCl, 0.2 mM EDTA, 0.5 mM PMSF, 0.5 mM DTT, 1× complete™ protease inhibitors). Nuclear proteins were extracted by the addition of 1/2 pnv high salt buffer (low salt buffer but 0.8 M KCl) and incubation at 4°C under constant mixing for 30 min. The extracted nuclei were pelleted for 20 min at 20 000*g* and 4°C. The supernatant was dialyzed against storage buffer (20 mM HEPES pH 8.0, 10% glycerol, 1.5 mM $MgCl_2$, 5 mM KCl, 0.2 mM EDTA, 0.5 mM PMSF, 0.5 mM DTT, 0.25× complete™ protease inhibitors). The dialyzed extracts were clarified by centrifugation for 20 min at 20 000*g* and 4°C and stored in aliquots at −80°C. Protein concentrations were estimated by the Bradford method (BioRad) using BSA as standard. Base release assays were then done according to (12) with slight modifications. An aliquot of 40 µl reactions contained 25 µg nuclear extracts and 1 pmol of either double-stranded homoduplex or mismatched DNA substrate (12). The reactions were incubated for 24 h at 37°C in reaction buffer (50 mM Tris-HCl

pH 8.0, 1 mM EDTA, 1 mM DTT, 1mg/ml BSA) containing 2 U UGI. Quantitative cleavage of AP sites was achieved by the addition of 100 mM NaOH and heating at 95°C for 10 min. Subsequently, DNA was ethanol precipitated overnight at −20°C in 0.3 M sodium acetate pH 5.2 and in the presence of 0.4 mg/ml carrier tRNA. The DNA was then pelleted by centrifugation (20 min, 20 000*g*, 4°C), washed once in 80% ethanol, air-dried, resuspended in formamide loading buffer (1× TBE, 90% formamide), heated at 95°C for 5 min and immediately chilled on ice. The reaction products were separated by electrophoresis in preheated 15% denaturing polyacrylamide gels and 1× TBE buffer. Visualization of the fluorescein labelled DNA was carried out on a Typhoon 9400 (GE Healthcare, Germany) and the data were quantified using the ImageQuant TL software (GE Healthcare, Germany).

RESULTS

S-phase progression requires cell cycle regulation of TDG-mediated BER

We found in different human cell models (HeLa, 293T, MRC5) that expression of high levels of TDG is incompatible with cell proliferation. Although transfection of various constructs designed for stable TDG expression produced transiently up to 30-fold the endogenous level, any attempt to maintain expression at levels above 5-fold in culture was unsuccessful. Cell cycle analyses then revealed that, following transfection with a TDG expressing construct, a fraction of cells accumulated specifically in S-phase of the cell cycle. This, however, was not observed in cell populations transfected with a catalytically inactive variant of TDG (Figure 1A), although transient expression levels were equally high. As previously observed (13), overexpressed TDG localized strictly to the cell nucleus (data not shown). Upon cultivation of the cells under conditions selecting for stable TDG expression, this cell cycle effect disappeared concomitantly with the drop of TDG protein to <5-fold the endogenous level (Figure 1B). These observations indicated that high levels of TDG lead to a disturbance of S-phase progression, thus conferring a selective advantage to low TDG expressing cells, i.e. the loss of high expressing cells, in the culture.

These findings prompted us to examine whether TDG expression underlies cell cycle regulation. To this end, we made use of two stably transfected HeLa cell populations, one expressing an N-terminally HA-tagged TDG from an SV40 promoter at ~5-fold the level of the endogenous protein (10), the other serving as a vector control and, thus, producing endogenous TDG only. We treated these cells with hydroxyurea (HU) or nocodazole (NO) to induce S- or G2/M-phase arrests, respectively, and then assessed TDG protein levels in denaturing cell extracts by immunoblotting with anti-TDG or anti-HA antibodies. To monitor the cell cycle status, we probed the membranes additionally with antibodies against cyclin E or cyclin B1 (Figure 2A). This showed that endogenous (Figure 2B) as well as ectopically expressed (Figure 2C) TDG was

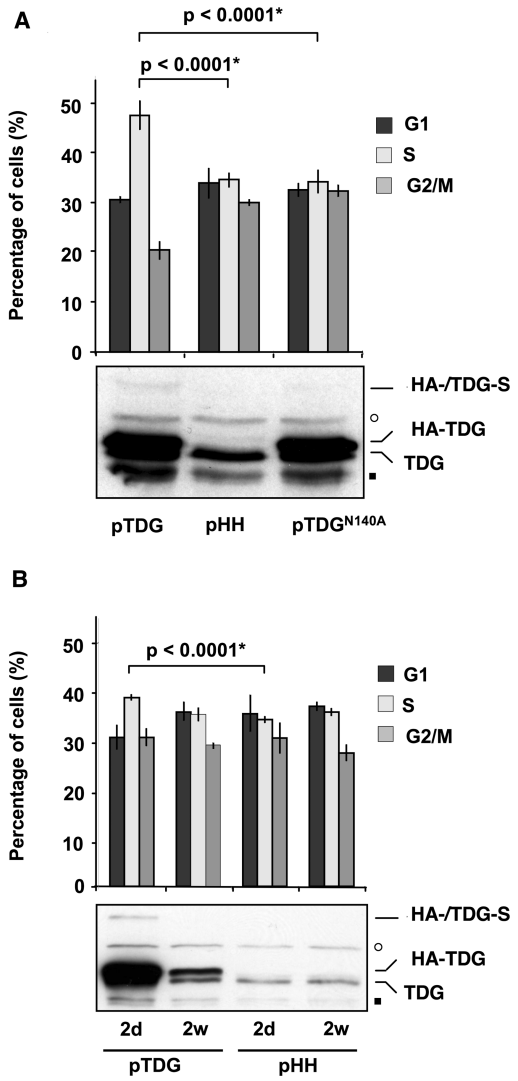

Figure 1. 293T cells expressing high levels of TDG accumulate in S-phase. (**A**) 293T cells were transiently co-transfected with a plasmid overexpressing either active HA-TDG (pTDG), the catalytically inactive variant HA-TDG/N140A (pTDG^{N140A}), or a vector control (pHH), and a EGFP expressing plasmid at a 10:1 ratio. The histogram shows the cell cycle distribution of transfected cells gated for EGFP positive cells, as determined by flow cytometry. The bottom panel documents TDG protein levels of the respective total cell population as determined by western blotting. TDG levels in cell populations carrying the overexpression construct were elevated by 20–30-fold. High levels of HA-TDG expression significantly increased the fraction of S-phase cells. This change in cell cycle distribution required TDG to be active, as overexpression of HA-TDG/N140A failed to produce the same effect. (**B**) The histogram shows the cell cycle distribution of 293T cells expressing active HA-TDG (pTDG) two days after transfection (2d) or after two weeks of selection for stable expression (2w). A vector control was also included (pHH). TDG expression levels are documented by western blots in the bottom panel. Shortly after transfection, TDG protein levels were 20–30 times higher than normal, but dropped to about three times the amount of endogenous TDG after selection. Concomitantly, the cell cycle effect seen after transfection disappeared. *P*-values (asterisk) were obtained by the Fisher's exact test from contingency tables comparing the distributions of G1-, S- and G2-cells. (Open circle) Unspecific cross-reaction of the primary antibody. (Filled square) Faster migrating forms of TDG. HA-/TDG-S: SUMO-modified HA-TDG and endogenous TDG, respectively.

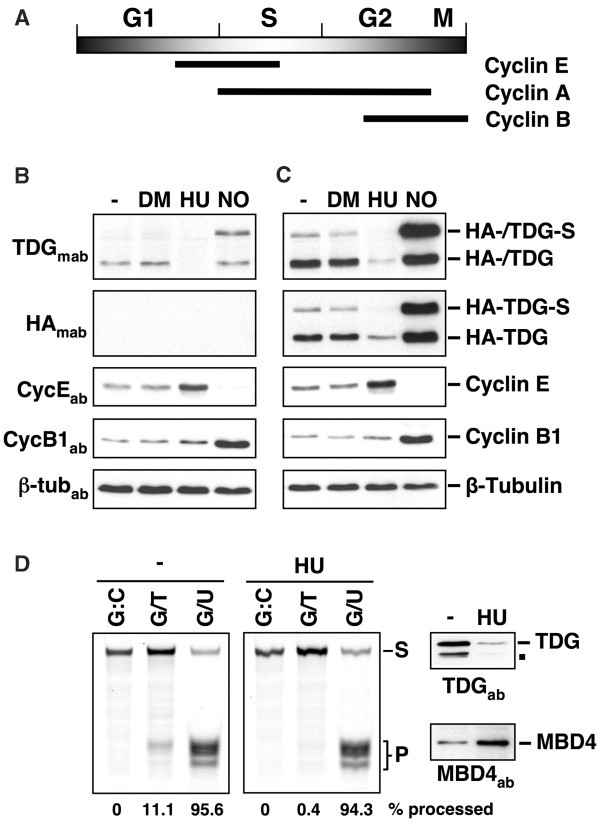

Figure 2. TDG is absent in S-phase arrested HeLa cells. (**A**) Schematic illustration of expression of cyclin E, cyclin A and cyclin B during the cell cycle. (**B** and **C**) HeLa cells expressing endogenous *TDG* alone or together with *HA-TDG* were blocked in S-phase with hydroxyurea (HU) or in G2/M with nocodazole (NO). Untreated asynchronous cells (-) and DMSO (DM) mock-treated cells were analysed in parallel. Denaturing cell extracts were examined by western blotting with antibodies against TDG or the HA-tag as indicated. Antibodies against Cyclin E and Cyclin B1 were applied to monitor the cell cycle arrest; β-tubulin staining served as a loading control. A monoclonal anti-TDG antibody (TDG_{mab}) detected endogenous TDG in extracts of untreated, mock treated or G2/M arrested cells, but none in extracts from S-phase arrested cells (B). Ectopically expressed HA-TDG also declined in HU arrested cells, although faint TDG (TDG_{mab}) and HA- (HA_{mab}) -specific signals were still discernible (C). (**D**) Base release assays with a fluorescent-labelled synthetic 60-mer DNA duplex document a significant reduction of G•T processing activity in nuclear extracts from HU-arrested HeLa cells. The assay was done with 25 µg of nuclear extract supplemented with 2 U of UNG2 inhibitory UGI peptide. A denaturing polyarcylamide gel with the intact DNA strand migrating at the top (S) and the cleaved products occurring as a consequence of G•T processing (P) are shown. Immunoblots of the corresponding cell extracts with TDG and MBD4-specific antibodies are shown on the right. (Filled square) Faster migrating forms of TDG. HA-/TDG-S: SUMO-modified HA-TDG and endogenous TDG, respectively.

virtually undetectable in S-phase arrested cells. Residual TDG signals likely reflected traces of protein from contaminating G2/M cells, as indicated by the low amounts of cyclin B1 in these extracts. Base excision assays with nuclear extracts (12) then revealed a >25-fold reduction of G•T glycosylase activity in HU-arrested HeLa cells (Figure 2D), and this correlated directly with the decline of TDG protein. MBD4, another mismatch-specific thymine-DNA glycosylase (5), did not contribute notably to G•T processing in these extracts (Figure 2D). Given the slight enrichment of the enzyme in S-phase arrested cells and that recombinant MBD4 is active under identical experimental conditions (data not shown), this must be interpreted to mean that G•T processing by BER is largely TDG dependent and does not occur during S-phase. By contrast, G•U processing did not correlate with TDG protein levels. Considering that these base release reactions were done in the presence of a 4-fold saturating amount of the UNG-inhibitory UGI peptide and that MBD4 appears to be poorly active in these extracts, the uracil processing observed in the S-phase arrested cells most likely reflected the activity of SMUG1. In the absence of the UGI-peptide, however, UNG2 was clearly the predominant uracil processing activity in these extracts (data not shown). Together, these experiments showed that HeLa cells down-regulate TDG protein and activity during S-phase and are able to do so even when it is stably expressed from an SV40 promoter at levels up to five times higher than normal.

To exclude that the HU treatment itself affects TDG stability, we examined its levels in synchronously cycling cell populations. Mitotic shake off experiments with HeLaS3 cells confirmed that TDG protein peaks during G1 and drops in S-phase (Figure 3A). Here, the disappearance of TDG coincided with the appearance of cyclin A (14), suggesting that downregulation occurs at the G1/S boundary. This experiment also confirmed the strict cell cycle regulation of the nuclear form of the highly efficient UNG (8,9) and thus, established that the expression of TDG and UNG2 is perfectly anti-cyclic with at most two short phases of overlap in late G1 and early G2 of the cell cycle.

Next, we performed immunofluorescence (IF) microscopy to correlate TDG expression with the PCNA status in an asynchronous HeLa cell population. This confirmed the absence of TDG from nuclei with focal PCNA pattern, i.e. from S-phase nuclei (Figure 3B). Ninety-two percent of cells with PCNA foci were TDG negative, whereas 96% of cells with diffuse PCNA staining had a strong nuclear TDG signal. Moreover, more than two-thirds of the nuclei with PCNA foci were in an early stage of DNA replication (15) and the vast majority of them (89%) were TDG negative. Together, these data establish that the decline of TDG in HeLa cells occurs at the G1–S transition, the latest in early S-phase.

Finally, we ascertained the cell cycle regulation of TDG in human primary fibroblasts. We synchronized MRC5 cells in early S-phase by serum starvation and mimosine treatment (16) and extracted protein and RNA from cells harvested at different time points following release into S-phase. Examination of the protein extracts by immunoblotting then showed that TDG was virtually undetectable at the mimosine block and for 10 h post-release (Figure 4A). According to the cyclin E and B1 expression patterns, this time period represented the progression of the cell population through S-phase. In G2, the TDG levels started to increase until they reached a maximum in the subsequent G1-phase. Examination of the steady-state levels of the *TDG* transcript by northern blotting showed only marginal fluctuations throughout

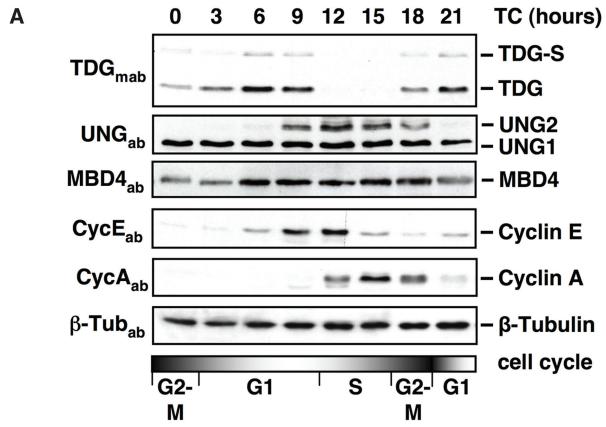

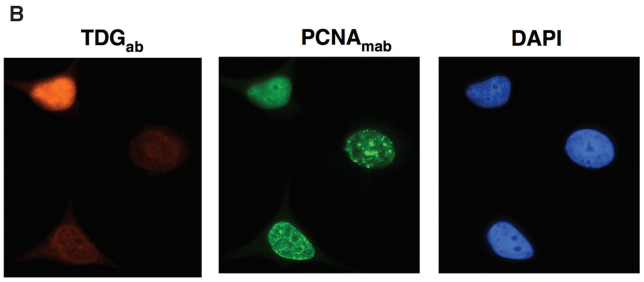

PCNA statu s	TDG positive		TDG negative		Total
	Cells	%	Cells	%	Cells
Diffuse PCNA (G1,G2/M)	320*	96.1	13*	3.9	333
Focal PCNA (S)	14*	8.4	153*	91.6	167
early S	13	11	104	89	117
mid S	0	0	40	100	40
late S	1	10	9	90	10

Figure 3. Cell cycle regulation of TDG in non-arrested cells. (**A**) HeLa S3 cells were synchronized by mitotic shake off. Following re-plating, TDG, UNG2 and MBD4 expression was examined in a time course (TC) of 21 h. At the time point indicated, cell extracts were prepared under denaturing conditions and analysed by western blotting with specific antibodies as indicated on the left. The cell cycle phases indicated at the bottom were deduced from the expression of cyclin A (S–G2/M) and E (G1–S). β-tubulin detection served as loading control. The monoclonal anti-TDG antibody detected TDG in mitotic and G1 cells (TC 0-9) and in G2/M cells (TC 18). No TDG was detectable in S-phase cells (TC 12,15). The disappearance of TDG at 12 h coincided with the *de novo* expression of cyclin A, indicating a downregulation of TDG at the G1/S boundary. By contrast, nuclear UNG2 was detectable between 9 and 18 h with a peak at 12 h, representing cells in S-phase. Mitochondrial UNG1 did not fluctuate throughout the cell cycle, nor did MBD4, which shows only slightly increased expression around S-phase. (**B**) Immunofluorescence staining of endogenous TDG and PCNA illustrate the absence of TDG from S-phase nuclei. Upper cell, TDG positive cell with diffuse PCNA staining; lower cell, TDG negative cell with PCNA staining indicating early to mid S-phase; middle cell, TDG negative cell with fewer and larger PCNA foci indicating late S-phase. Shown are typical events of 500 randomly chosen cells scored and classified as indicated in the table at the bottom. Asterisk: statistically significant difference, $P<0.0001$ by contingency tables and Fisher's exact test; TDG-S: endogenous TDG modified with SUMO.

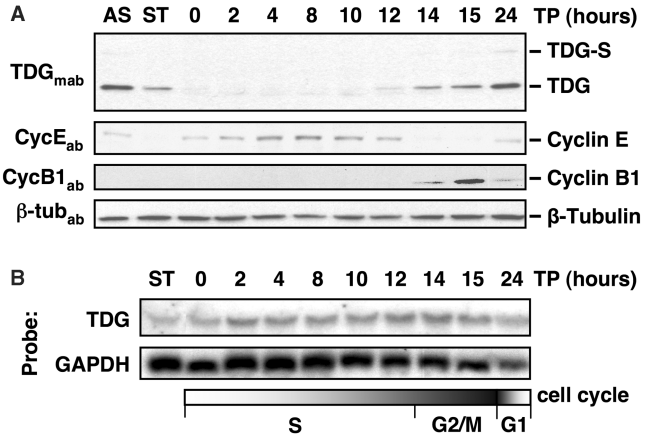

Figure 4. TDG protein levels fluctuate during the cell cycle in primary cells but mRNA is constitutively transcribed. MRC5 primary fibroblasts were synchronized in early S-phase by serum starvation and mimosine treatment. (**A**) Western blot analyses of protein extracts prepared from asynchronous cells (AS), serum starved cells (ST) and cells harvested at indicated times (TP hours) after release from the mimosine block. Proteins examined were endogenous TDG, Cyclin E, Cyclin B1 and β-tubulin as a loading control. TDG-specific signals appeared at 12 h after release into S-phase and increased gradually to the levels found in the asynchronous culture. Expression of cyclin E and cyclin B1 coincided with the lack or the presence of TDG, respectively. (**B**) Northern blot analysis of TDG and GAPDH mRNAs (loading control) at corresponding time points, showing that TDG-specific mRNA was detectable throughout the cell cycle. TDG-S: endogenous TDG modified with SUMO.

the cell cycle (Figure 4B), which cannot account for the dramatic changes seen at the protein level. Hence, cell-cycle-dependent expression of TDG applies to different human cell types and does not involve regulation at the levels of promoter activity or mRNA stability.

TDG is targeted by ubiquitin for proteasomal degradation

We then addressed a possible role of posttranslational modifications in the regulation of TDG. To examine whether the glycosylase is subject to degradation by the ubiquitin–proteasome system (17), we measured the effect of MG132, a reversible inhibitor of the 26S proteasome, on the TDG protein level in asynchronously proliferating HeLa cells. Cells treated with MG132 had clearly elevated steady-state levels of TDG (Figure 5A). This effect, however, was only apparent when extracts were prepared under denaturing conditions, the reason being a change in TDG solubility upon proteasome inhibition. While TDG extracted predominantly in the soluble protein fraction in untreated cells, a substantial amount became insoluble after MG132 treatment (Figure S1A), just like the majority of ubiquitin-conjugated proteins (Figure S2B). Following these indications for ubiquitylation of TDG, we prepared denaturing extracts from HeLa cells, again expressing either endogenous TDG alone or together with HA-TDG, for immunoprecipitation (IP). IP with an affinity-purified polyclonal TDG antibody then led to the expected enrichment of the glycosylase as evident from immunoblotting with a monoclonal TDG antibody (Figure 5B, left panel). The same antibody, however,

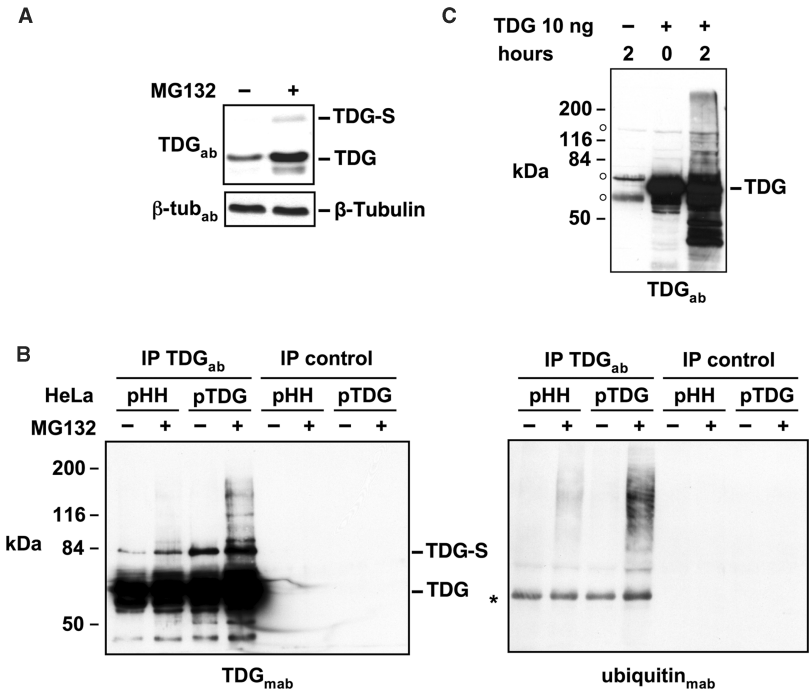

Figure 5. TDG is polyubiquitylated and stabilized by proteasome inhibition. (**A**) Asynchronous HeLa cultures were treated with the proteasome inhibitor MG132 (20 μM) or DMSO. Cell extracts prepared under denaturing conditions were analysed by western blotting with a polyclonal anti-TDG (TDG$_{ab}$) and an anti-β-tubulin antibody (β-tub$_{ab}$). SUMOylated and unmodified TDG increased after proteasome inhibition. (**B**) HeLa cells stably transfected with a HA-TDG (pTDG) expression construct or the vector (pHH) were treated with MG132 or DMSO. Cell extracts prepared under denaturing conditions were subjected to TDG-IP with an affinity purified polyclonal anti-TDG antibody (TDG$_{ab}$). Bound protein fractions were analysed by western blotting with the monoclonal anti-TDG (TDG$_{mab,}$ left panel) or an anti-ubiquitin antibody (ubiquitin$_{ab}$, right panel). Strong signals appeared in the TDG-IPs but none in the IP-controls. TDG-specific signals smearing towards higher molecular weights indicated an accumulation of modified TDG in extracts of MG132 treated cells. The anti-ubiquitin antibody detected proteins with comparable migration properties in the corresponding TDG-IP protein fractions. (**C**) 10 ng of purified recombinant TDG were subjected to *in vitro* ubiquitylation. Shown is a western blot with the polyclonal anti-TDG antibody of aliquots taken at 0 and 2 h of incubation, and of a control reaction lacking TDG. The appearance of TDG-dependent high molecular weight bands after 2 h indicates ubiquitylation of TDG. (Asterisk), protein co-precipitating in TDG-IP and cross-reacting with the secondary antibody used; (Open circle) Components of the ubiquitylation system cross-reacting with the anti-TDG antibody.

also detected a smear of high molecular weight proteins in the TDG-IP's from extracts of proteasome inhibited cells. These signals were more pronounced in the extracts containing additional HA-TDG. Probing of the membrane with a specific anti-ubiquitin antibody revealed proteins at high molecular weight, resembling the pattern observed with the TDG antibody (Figure 5B, right panel). Thus, polyubiquitylated protein species co-precipitated with a TDG-specific antibody from extracts of proteasome inhibited cells. Unspecific binding of ubiquitylated proteins to the beads did not occur (see control IP), and, given the denaturing conditions applied for extract preparation, unspecific binding of ubiquitylated proteins to TDG can also be virtually excluded. We therefore conclude that the proteins recognized by the anti-ubiquitin antibody must be TDG isoforms carrying polyubiquitin chains of different lengths. To formally prove its susceptibility to ubiquitin conjugation, we subjected bacterially produced TDG to ubiquitylation in an *in vitro* reconstituted assay. This indeed produced TDG isoforms of increased molecular weight (Figure 5C). The reaction, however, was inefficient, indicating that ubiquitylation *in vivo* may require priming of TDG, possibly by phosphorylation, to stimulate its interaction with an E3 ubiquitin ligase (18). Taken together, our data strongly suggest that polyubiquitylation and proteasomal degradation is the mechanism underlying the disappearance of TDG at the G1/S boundary of the cell cycle. TDG was also shown to be target for SUMO conjugation in cells (10). To address whether SUMO modification contributes to the cell cycle regulation of TDG, we examined the behaviour of an ectopically expressed SUMOylation-deficient TDG variant (HA-TDG^{K330A}) upon HU or NO treatment of the cells. The protein was absent from S-phase cells and enriched at the G2/M stage, exactly as the wild-type control (Figure S1C), establishing that SUMO modification neither positively nor negatively interferes with TDG ubiquitylation and proteasome degradation.

DISCUSSION

Our data establish that two prominent members of the UDG family, TDG and UNG2, underlie strict anticyclic cell cycle regulation. While TDG is highly expressed throughout the G2-M and G1 phases its levels rapidly

decline at the G1–S transition just when UNG2 starts to rise above background. The UNG2 protein then peaks at the beginning of S-phase and gradually declines towards termination of DNA replication (see also reference 9), when TDG expression resumes. This implicates that the two biochemically redundant UDGs control non-redundant, cell cycle stage-specific pathways for uracil repair; while UNG2 is active during DNA replication, TDG functions in non-replicating DNA, notably, when U arises mainly through deamination of cytosine. Strikingly, although the pattern of cell cycle regulation of the two UDGs is diametrically opposed, the underlying mechanism appears to be the same. As shown here for TDG and reported previously for UNG2 (9), both are subject to cell cycle controlled ubiquitylation and proteasome degradation. Thus, the ubiquitin–proteasome system appears to be at the heart of the coordination of redundant BER pathways, which would be an as yet unrecognized function. Whether this interesting concept of coordination is a feature restricted to TDG and UNG2 only, or whether it applies more generally to DNA repair remains to be resolved.

We wanted to get some insight into why TDG needs to be eliminated before S-phase from ectopically expressing the glycosylase to levels saturating its degradation. TDG expression at >30-fold the endogenous level could readily be obtained by transient transfection, and such amounts were indeed saturating in the sense that low amounts of the protein remained detectable in S-phase arrested cell populations. Yet, attempts to maintain high expression in culture failed; upon selection of stable clones, TDG expression declined to levels <5-fold that were compatible with complete degradation of the protein in S-phase. Thus, the presence of TDG in S-phase seems incompatible with cell cycle progression and proliferation, and this is in line with the observation that 293T cells transiently expressing high levels of wild-type TDG accumulate in S-phase.

Interference with S-phase progression might occur at the level of U excision (1). If misincorporated, U must be eliminated from newly synthesized DNA in a way that is coordinated with the replication process. Given its enzymatic properties, TDG would be totally unsuited for this task; by processing A•U only inefficiently (19) and binding to AP sites with high affinity (10,20), it would perturb the replication process. By contrast, UNG2 would be the glycosylase of choice here; it processes U•A with a comparably high rate, and it associates with replication factors at the replication fork. Consistently, UNG was shown to keep genomic uracil levels low (1,8,21,22).

Considering the rather broad substrate spectrum of TDG (19), however, its presence in S-phase might cause other forms of interference. TDG could induce the formation of DNA double-strand breaks either directly, if it removed substrate bases close to each other in opposite DNA strands, or indirectly, through the generation of replication blocking lesions such as AP sites or single-strand breaks. The latter would be aided by the inability of TDG to dissociate freely from AP sites (12,20). *In vitro*, AP-site release is facilitated by a SUMOylation-induced conformational change in TDG, a rate-limiting step that appears useful for a temporary protection of the labile intermediate in the repair process (10,23). The protective nature of this dissociation delay, however, may turn into a disadvantage in the context of DNA replication; it might generate situations where TDG is bound to AP sites in front of an approaching replication fork where it acts as a road block, causing fork stalling and eventually collapse.

A special case of mutagenic interference during S-phase may relate to TDG's ability to remove T from G•T mismatches. While this feature provides an excellent means to counter mutagenesis by deamination of 5-meC, it may represent a disadvantage during DNA replication, where G•T mispairs arise predominantly by DNA polymerase errors. The inability of TDG to discriminate between parental and newly synthesized DNA strands would fix C to T transition mutations in cases where the T is in the parental strand. In addition, TDG induced postreplicative G•T repair in the parental DNA strand, particularly in the parental lagging strand, could destabilize the replication fork and thereby impede the replication process. Thus, G•T correction during DNA synthesis should be left to the postreplicative mismatch repair system, which is designed to correct the error in the newly synthesized DNA strand.

SUPPLEMENTARY DATA

Supplementary Data are available at NAR Online.

ACKNOWLEDGEMENTS

Thanks go to Josef Jiricny, Stefano Ferrari, Giancarlo Marra and Teresa Lettieri for stimulating discussions and support, and to Margaret Fäsi for excellent technical assistance. This study was funded by grants from the Swiss National Science Foundation (U.H., C.K) and the Schweizerische Krebsliga (U.H.). Funding to pay the Open Access publication charges for this article was provided by the University of Basel.

Conflict of interest statement. None declared.

REFERENCES

1. Krokan,H.E., Drablos,F. and Slupphaug,G. (2002) Uracil in DNA – occurrence, consequences and repair. *Oncogene*, **21**, 8935–8948.
2. Barnes,D.E. and Lindahl,T. (2004) Repair and genetic consequences of endogenous DNA base damage in mammalian cells. *Annu. Rev. Genet.*, **38**, 445–476.
3. Slupphaug,G., Eftedal,I., Kavli,B., Bharati,S., Helle,N.M., Haug,T., Levine,D.W. and Krokan,H.E. (1995) Properties of a recombinant human uracil-DNA glycosylase from the UNG gene and evidence that UNG encodes the major uracil-DNA glycosylase. *Biochemistry*, **34**, 128–138.
4. Haushalter,K.A., Todd Stukenberg,M.W., Kirschner,M.W. and Verdine,G.L. (1999) Identification of a new uracil-DNA glycosylase family by expression cloning using synthetic inhibitors. *Curr. Biol.*, **9**, 174–185.
5. Hendrich,B., Hardeland,U., Ng,H.H., Jiricny,J. and Bird,A. (1999) The thymine glycosylase MBD4 can bind to the product of deamination at methylated CpG sites. *Nature*, **401**, 301–304.

6. Hardeland,U., Bentele,M., Lettieri,T., Steinacher,R., Jiricny,J. and Schär,P. (2001) Thymine DNA glycosylase. *Prog. Nucleic Acid Res. Mol. Biol.*, **68**, 235–253.
7. Nilsen,H., Otterlei,M., Haug,T., Solum,K., Nagelhus,T.A., Skorpen,F. and Krokan,H.E. (1997) Nuclear and mitochondrial uracil-DNA glycosylases are generated by alternative splicing and transcription from different positions in the UNG gene. *Nucleic Acids Res.*, **25**, 750–755.
8. Otterlei,M., Warbrick,E., Nagelhus,T.A., Haug,T., Slupphaug,G., Akbari,M., Aas,P.A., Steinsbekk,K., Bakke,O. *et al.* (1999) Post-replicative base excision repair in replication foci. *EMBO J.*, **18**, 3834–3844.
9. Fischer,J.A., Muller-Weeks,S. and Caradonna,S. (2004) Proteolytic degradation of the nuclear isoform of uracil-DNA glycosylase occurs during the S phase of the cell cycle. *DNA Repair (Amst.)*, **3**, 505–513.
10. Hardeland,U., Steinacher,R., Jiricny,J. and Schär,P. (2002) Modification of the human thymine-DNA glycosylase by ubiquitin-like proteins facilitates enzymatic turnover. *EMBO J.*, **21**, 1456–1464.
11. Szadkowski,M. and Jiricny,J. (2002) Identification and functional characterization of the promoter region of the human MSH6 gene. *Genes Chromosomes Cancer*, **33**, 36–46.
12. Hardeland,U., Bentele,M., Jiricny,J. and Schär,P. (2000) Separating substrate recognition from base hydrolysis in human thymine DNA glycosylase by mutational analysis. *J. Biol. Chem.*, **275**, 33449–33456.
13. Mohan,R.D., Rao,A., Gagliardi,J. and Tini,M. (2007) SUMO-1-dependent allosteric regulation of thymine DNA glycosylase alters subnuclear localization and CBP/p300 recruitment. *Mol. Cell. Biol.*, **27**, 229–243.
14. Yam,C.H., Fung,T.K. and Poon,R.Y. (2002) Cyclin A in cell cycle control and cancer. *Cell. Mol. Life Sci.*, **59**, 1317–1326.
15. Leonhardt,H., Rahn,H.P., Weinzierl,P., Sporbert,A., Cremer,T., Zink,D. and Cardoso,M.C. (2000) Dynamics of DNA replication factories in living cells. *J. Cell. Biol.*, **149**, 271–280.
16. Gilbert,D.M., Neilson,A., Miyazawa,H., DePamphilis,M.L. and Burhans,W.C. (1995) Mimosine arrests DNA synthesis at replication forks by inhibiting deoxyribonucleotide metabolism. *J. Biol. Chem.*, **270**, 9597–9606.
17. Nandi,D., Tahiliani,P., Kumar,A. and Chandu,D. (2006) The ubiquitin-proteasome system. *J. Biosci.*, **31**, 137–155.
18. Gao,M. and Karin,M. (2005) Regulating the regulators: control of protein ubiquitination and ubiquitin-like modifications by extracellular stimuli. *Mol. Cell*, **19**, 581–593.
19. Hardeland,U., Bentele,M., Jiricny,J. and Schär,P. (2003) The versatile thymine DNA-glycosylase: a comparative characterization of the human, Drosophila and fission yeast orthologs. *Nucleic Acids Res.*, **31**, 2261–2271.
20. Waters,T.R., Gallinari,P., Jiricny,J. and Swann,P.F. (1999) Human thymine DNA glycosylase binds to apurinic sites in DNA but is displaced by human apurinic endonuclease 1. *J. Biol. Chem.*, **274**, 67–74.
21. Akbari,M., Otterlei,M., Pena-Diaz,J., Aas,P.A., Kavli,B., Liabakk,N.B., Hagen,L., Imai,K., Durandy,A. *et al.* (2004) Repair of U/G and U/A in DNA by UNG2-associated repair complexes takes place predominantly by short-patch repair both in proliferating and growth-arrested cells. *Nucleic Acids Res.*, **32**, 5486–5498.
22. Nilsen,H., Rosewell,I., Robins,P., Skjelbred,C., Andersen,S., Slupphaug,G., Daly,G., Krokan,H.E., Lindahl,T. *et al.* (2000) Uracil-DNA glycosylase (UNG)-deficient mice reveal a primary role of the enzyme during DNA replication. *Mol. Cell*, **5**, 1059–1065.
23. Steinacher,R. and Schär,P. (2005) Functionality of human thymine DNA glycosylase requires SUMO-regulated changes in protein conformation. *Curr. Biol.*, **15**, 616–623.